Povezivanje u spoju mortom u ziđu od opečnih blokova

Penava, Davorin; Sigmund, Vladimir; Kožar, Ivica; Anić, Filip; Trajber, Domagoj; Vig, Mirko

Source / Izvornik: **Građevinar, 2016, 68, 609 - 616**

Journal article, Published version
Rad u časopisu, Objavljena verzija rada (izdavačev PDF)

https://doi.org/10.14256/JCE.1576.2016

Primljen / Received: 23.1.2016.
Ispravljen / Corrected: 14.7.2016.
Prihvaćen / Accepted: 23.8.2016.
Dostupno online / Available online: 10.9.2016.

Clay block masonry and mortar joint interlocking

Authors:

[1] Assist.Prof. **Davorin Penava**
davorin.penava@gfos.hr

[1] Prof. **Vladimir Sigmund**

[2] Prof. **Ivica Kožar**
ivica.kozar@uniri.hr

[1] **Filip Anić**, MCE
filip.anic@gfos.hr

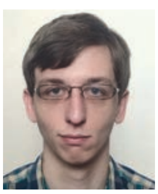

[1] **Domagoj Trajber**, MCE
domagoj.trajber@gfos.hr

[1] **Mirko Vig**, MCE
mirko.vig@gfos.hr

[1] University of J.J. Strossmayer in Osijek
Faculty of Civil Engineering Osijek

[2] University of Rijeka
Faculty of Civil Engineering

Original scientific paper

Davorin Penava, Vladimir Sigmund, Ivica Kožar, Filip Anić, Domagoj Trajber, Mirko Vig

Clay block masonry and mortar joint interlocking

If clay blocks with vertical voids and general-purpose mortar are used in masonry construction, interlocking will occur during placement of units and mortar. Shear strength of the clay block and solid brick masonry is usually determined in the same way, without taking interlocking into consideration. With interlocking, the tensile strength of clay blocks is reached before mortar bed joint sliding occurs. In order to consider the effect of interlocking in nonlinear analyses, three-dimensional design models were built and verified using physical model response. The shear resistance function was adopted to enable proper description of masonry response.

Ključne riječi:

clay block masonry, masonry shear strength, nonlinear design model, shear resistance function

Izvorni znanstveni rad

Davorin Penava, Vladimir Sigmund, Ivica Kožar, Filip Anić, Domagoj Trajber, Mirko Vig

Povezivanje u spoju mortom u zidu od opečnih blokova

Ako se pri izvedbi konstrukcijskog zida upotrebljavaju opečni zidni elementi s vertikalnim šupljinama i mort opće namjene, tijekom ispunjavanja sljubnica nastupa prodiranje morta u šupljine zidnog elementa. Otpornost pri posmiku određuje se na jednak način za zide od punih ili šupljih opečnih zidnih elemenata te stoga utjecaj međusobnog spoja zidnih elemenata i sljubnica morta nije uzet u obzir. Pomoću prostornih nelinearnih proračunskih modela i usporedbom s odzivom fizikalnih modela provjeren je utjecaj međusobnog spoja šupljih zidnih elemenata i sljubnica morta na posmičnu nosivost.

Ključne riječi:

šuplji opečni zidni elementi, posmična čvrstoća zida, nelinearni proračunski model, funkcija otpornosti pri posmiku

Wissenschaftlicher Originalbeitrag

Davorin Penava, Vladimir Sigmund, Ivica Kožar, Filip Anić, Domagoj Trajber, Mirko Vig

Blockziegelmauerwerk und Verbund an der Mörtelfuge

Wenn für tragendes Mauerwerk Blockziegel und Allzweckmörtel verwendet werden, kommt es bei der Ausführung zur Verknüpfung von Ziegelsteinen und Mörtel. Der Schubwiderstand wird normalerweise gleicherweise für Mauerwerk aus Hohlziegel und für Vollsteinmauerwerk ermittelt, so dass Einflüsse der gegenseitigen Verbindung nicht berücksichtigt werden. Aufgrund der Verknüpfung wird der Zugwiderstand der Blockziegel erreicht, bevor der Schubwiderstand der Mörtelfuge ausgeschöpft ist. Um den Effekt der Wechselwirkung in nichtlinearen Analysen zu berücksichtigen, wurden dreidimensionale Berechnungsmodelle aufgestellt und aufgrund physischen Modellverhaltens verifiziert. Die Schubwiderstandsfunktion wurde eingeführt, um das Verhalten des Mauerwerks auf geeignete Weise darzustellen.

Ključne riječi:

Wandelement aus Hohlziegel, Schubwiderstand von Mauerwerk, nichtlineares Berechnungsmodell, Widerstandsfunktion bei Schubeinwirkungen

1. Introduction

Interlocking will occur if clay blocks are used in masonry construction (Figure 1) during placement of units and mortar. In the design of masonry structures presented in [1-3], shear strength is determined under assumption of the same masonry bond along mortar bed joints for clay block and solid brick masonry, i.e., $f_v = f_{v0} + \mu \cdot f_p$, where f_{v0} is the initial shear strength, μ is the coefficient of internal friction and f_p is the compressive stress. Therefore, the influence of interlocking is not considered. Additionally, the limit to the shear strength value is set to the masonry unit tensile strength normal to the bed face, i.e., $f_{vlt} = f_{mu,t,h} = 0.065 \cdot f_{mu,c,h}$, where $f_{mu,c,h}$ is the corresponding masonry unit compressive strength. Thus, physical properties of the clay blocks parallel to the bed face, e.g., $f_{mu,c,b}$, are not accounted for, with the exception of $f_{mu,c,b,min} = 2$ N/mm² according to [2]. The influence of interlocking on the shear strength of the clay block masonry was investigated in this paper. Tests were conducted along the mortar head and bed joints with and without interlocking, respectively. Physical properties of the clay blocks normal and parallel to the bed face were determined in compliance with [5, 6]. Masonry specimens (physical models) for shear strength tests were built according to [7]. Physical properties of clay blocks and masonry bond were used to build three-dimensional design models in a computer program [8] in order to adequately present interlocking in non-linear analyses. The shear strength of clay block masonry was equal to the tensile strength of clay blocks parallel to the bed face. The interlocking of mortar bed joints in the design model was successfully described by the shear resistance function.

Figure 1. Clay block masonry infill construction as per [4]

Table 1. Mean properties of clay block masonry units parallel and normal to the bed face

Description	Symbol	Value	Units
Compressive strength parallel to voids	$f_{mu.c.h}$	14.79	N/mm²
Compressive strength perpendicular to voids	$f_{mu.c.b}$	3.49	N/mm²
Tensile strength parallel to voids	$f_{mu.t.h}$	$0.065 \cdot f_{mu.c.h}$	N/mm²
Tensile strength perpendicular to voids	$f_{mu.t.b}$	$0.065 \cdot f_{mu.c.b}$	N/mm²
Modulus of elasticity parallel to voids	$E_{mu.t.h}$	4002	N/mm²
Modulus of elasticity perpendicular to voids	$E_{mu.t.b}$	949	N/mm²
Ultimate strain parallel to voids	$\varepsilon_{mu.t.h}$	3.70	‰
Ultimate strain perpendicular to voids	$\varepsilon_{mu.t.b}$	3.64	‰
Poisson's ratio parallel to voids	$\upsilon_{mu.c.h}$	0.10	-
Poisson's ratio perpendicular to voids	$\upsilon_{mu.c.b}$	$\upsilon_{mu.c.h} \cdot E_{mu.t.b} / E_{mu.t.h}$	-
Net density	ρ_{nu}	0.760	g/mm³

2. Clay block masonry

The masonry units used in this study had a length of l_{mu} = 250 mm, width of w_{mu} = 120 mm, and a height of h_{mu}=65 mm, in compliance with [5, 9], as shown in detail in Figure 2.

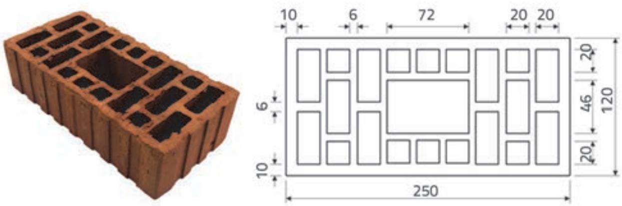

Figure 2. Clay block masonry unit used in this study (dimensions in mm)

The volume of voids compared to the total volume of the unit was V_{vu} / V_{gu} · 100 = 68 %, determined in compliance with [10]. Physical properties, normal and parallel to the bed face, were determined in compliance with [5, 6] and are shown in Table 1. According to requirements specified in [2], only mean properties were considered.

3. Shear strength tests

Clay block masonry specimens (physical models) were built in compliance with [1, 7]. Clay blocks were laid with general purpose mortar (with proportions by volume of cement, lime and sand of 1:1:5, respectively) of class M5 as required by [2] and determined in compliance with [11]. During the placement of clay blocks and mortar, interlocking occurred due to voids in the masonry units along mortar bed joints (Figure 3.a) but not along head joints (Figure 3.b).

3.1. Masonry bond without interlocking

Tests along mortar head joints were conducted under the compressive stress of f_p = 0.2, 0.6 and 1.0 N/mm^2. During the tests, the mortar head joint sliding occurred as shown in Figure 4. In compliance with tests results presented in Figure 5, the initial shear strength of mortar head joints was determined as $f_{v0,h}$ = 0.05 N/mm^2 and the coefficient of internal friction as μ_h = 0.45.

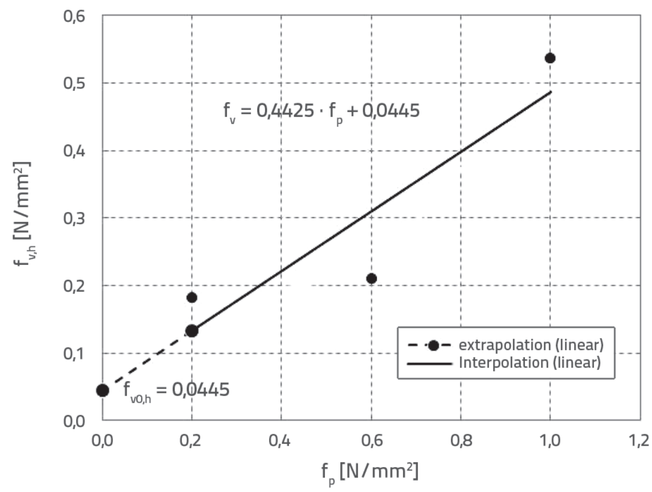

Figure 5. Results for shear strength tests along mortar head joints

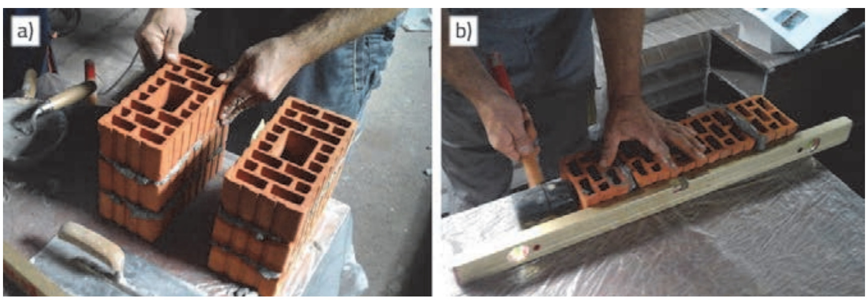

Figure 3. Preparation of clay block masonry specimens for shear strength tests along mortar: a) bed; b) head joints

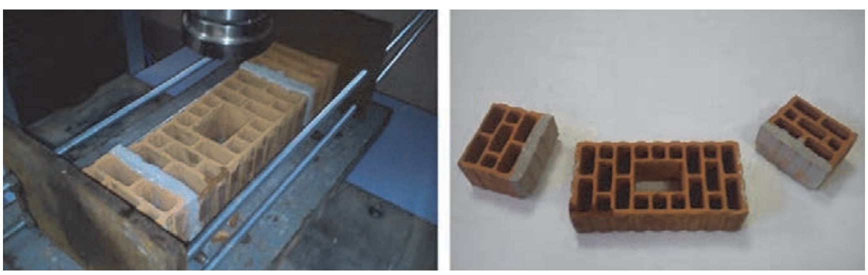

Figure 4. Mortar head joint sliding failure

3.2. Masonry bond with interlocking

Tests along mortar bed joints were conducted without compressive stress, i.e., f_p = 0. During tests, the tensile strength of the masonry units, i.e., $f_{mu,t,b}$ was reached before the mortar bed joint sliding occurred, i.e., before $f_{v0,b}$ could occur (Figure 6). The ultimate shear stress amounted to f_{vi} = 0.22 N/mm^2 (Figure 7), this corresponded well with the value gained by the expression f_{vlt} = $f_{mu,t,b}$ = 0.065· $f_{mu,c,b}$, where $f_{mu,c,b}$ is the clay block compressive strength parallel to the bed face (Table 1).

Figure 6. Clay block tensile failure due to masonry bond with interlocking

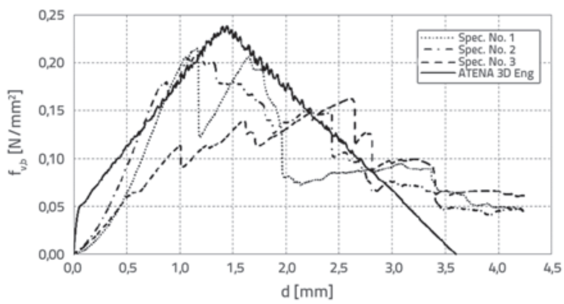

Figure 7. Results of shear strength tests along mortar bed joints

4. Three-dimensional computational model

Three-dimensional non-linear finite element models and the ATENA 3D Eng computer program were employed in order to mathematically describe the influence of interlocking along mortar joints [8]. The models were built to match physical models.

4.1. Clay block

As their physical properties are different parallel and perpendicular to voids (see Table 1), clay blocks were modelled as a composite of two materials, as shown in Figure 8.

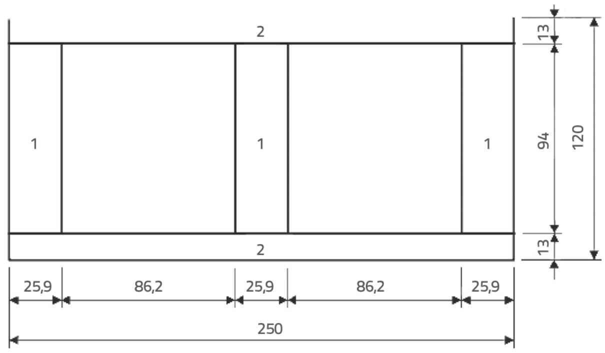

Figure 8. Clay block composite model

The CC3DNonLinCementitious2 (see Figure 9) constitutive material model was adopted In compliance with [12], and its physical properties are presented in Table 2. This is a fracture-plastic model that combines constitutive models for tensile (fracturing) and compressive (plastic) behaviour [12]. Clay block modelling is elaborated in detail in [13,14]. CCIsoBrick elements were used.

4.2. Masonry bond

Masonry mortar bed and head joints were modelled using the interface material model and CCIsoGap finite elements of zero thickness [12]. The interface material is based on the Mohr-Coulomb criterion with tension cut-off (see Figure 10).

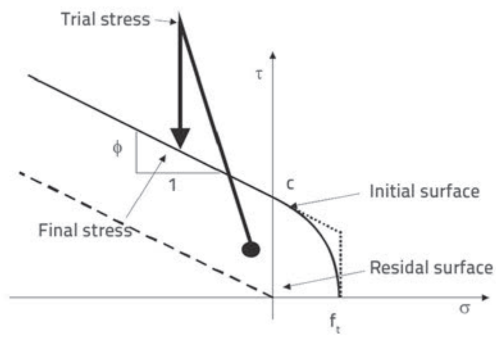

Figure 10. Mohr-Coulomb criterion with tension cut-off in Interface Material Model

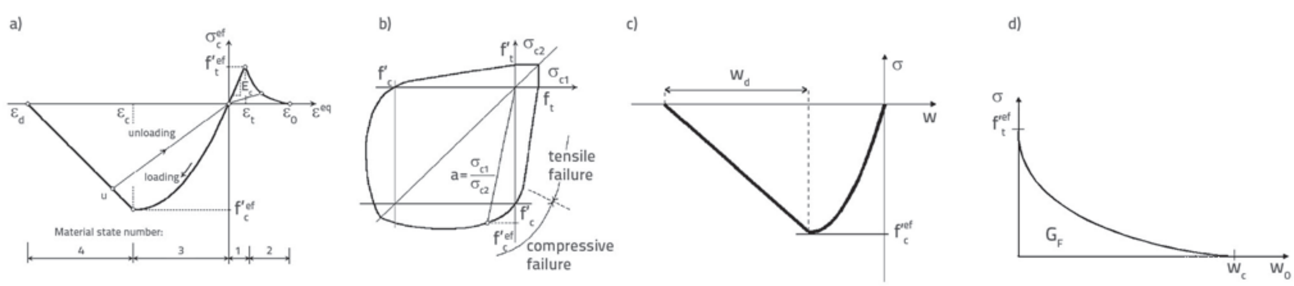

Figure 9. CC3DNonLinCementitious2 constitutive material model: a) stress-strain law; b) biaxial failure law; c) compression; d) tension after peak stress

Table 2. Physical properties of clay block constitutive model CC3DNonLinCementitious2

Description	Symbol	Material 1	Material 2	Units
Elastic modulus	E	12469.25	4428.08	N/mm^2
Poisson's ratio	μ	0.100	0.035	-
Tensile strength	f_t	3.00	1.05	N/mm^2
Compressive strength	f_c	-46.21	-16.10	N/mm^2
Specific fracture energy	G_F	$7.509 \cdot 10^{-2}$	$2.616 \cdot 10^{-2}$	N/mm
Critical compressive displacement	w_d	-0.01	-0.5	mm
Plastic strain at compressive strength	ε_{cp}	$-1.00 \cdot 10^{-8}$	$-1.00 \cdot 10^{-8}$	-
Reduction of comp. strength due to cracks	$r_{c.lim}$	0.80	0.80	-
Crack shear stiff. factor	s_F	20	20	-
Failure surface eccentricity	-	0.520	0.520	-
Multiplier for plastic flow direction	β	0.00	0.00	-
Specific material weight	ρ	$0.0239 \cdot 10^{-3}$	$0.0239 \cdot 10^{-3}$	N/mm^3
Coefficient of thermal expansion	α	$1.20 \cdot 10^{-5}$	$1.20 \cdot 10^{-5}$	1/C
Fixed crack model coefficient	-	0	0	-

Table 3. Physical properties of mortar joint constitutive interface material model

Description	Symbol	Material 1	Material 2	Units
Normal stiffness	K_{nn}	1249.16	442.52	N/mm^3
Tangential stiffness	K_{tt}	567.80	213.69	N/mm^3
Tensile strength	f_t	0.17	0.17	N/mm^2
Cohesion	c	0.10	0.10	N/mm^2
Friction coefficient	-	0.44	0.44	-
Minimal normal stiffness for numerical purposes	$K_{nn.min}$	1.25	0.44	N/mm^3
Minimal tangential stiffness for numerical purposes	$K_{tt.min}$	0.57	0.21	N/mm^3

Physical properties of head joints were adopted for mortar joints, i.e., $f_{v0,b} = f_{v0,h}$ and $\mu_b = \mu_h$. The tensile strength of $f_{t,b} = f_{t,h} = 0.08$ N/mm² was taken from [15]. Values had to be adapted to the net area of the clay block model, since they were expressed as gross values as described in [13, 14]. These values are shown in Table 3.

To include the influence of interlocking in the model, mortar bed joints were supplemented with the shear resistance function shown in Figure 11. The function was created based on observations of shear strength tests along mortar bed joints, as shown in Figure 7.

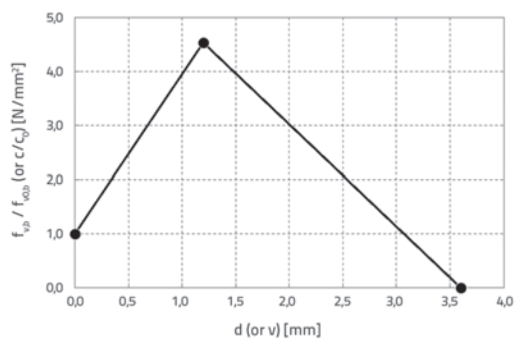

Figure 11. Shear strength function

The shear resistance function consisted of three points with shear strength f_v / N/mm² on the ordinate and displacement d / mm on the abscissa (c/c_0 and v in ATENA 3D Eng):
- first point $f_v = f_{v0,b} / f_{v0,b} = 1$ and $d_1 = 0$
- second point $f_v = f_{mu,t,b} / f_{v0,b} = 4.54$ and $d_2 = 1.2$ mm
- third point $f_v = 0 / f_{v0,b} = 0$ and $d = 3 \cdot d_2 = 3.6$ mm

Normal and shear stiffness of the interface, K_{nn} and K_{tt}, respectively, (Table 3) were evaluated in compliance with [12-14] using t = 10 mm.

4.3. Model verification

The sensitivity of the computational model with respect to the finite element mesh density was analysed using the finite element sizes of 10, 20 and 30 mm (Tables 4 and 5). Additionally, the loading increment size was considered using the prescribed displacement step of 0.01 or 0.02 mm.

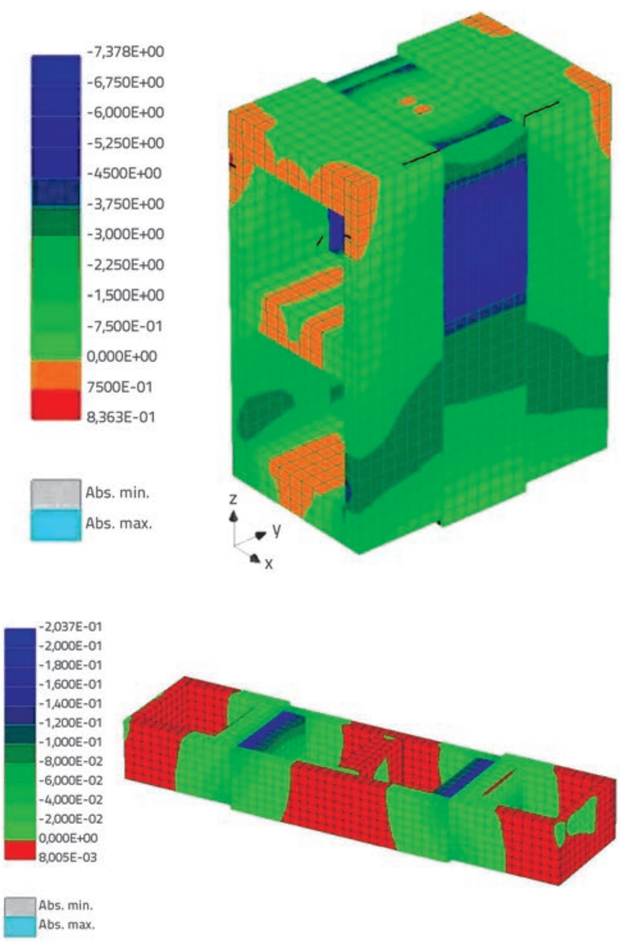

Figure 12. Clay block normal stress parallel (up) and normal (down) to bed face (in N/mm²).

The resulting response along mortar bed joints in the form of shear stress and displacement relation is shown in Figure 7, parallel to test results. Normal stress in clay blocks in a state of near collapse (finite element mesh size of 10 mm and a prescribed displacement step of 0.01 mm) is shown in Figure12, parallel to the direction of the shear strength test simulation. In the shear strength test simulation along mortar bed joints (Figure 12), the tensile stress in clay blocks parallel to the bed face was roughly 0.75 N/mm². In the case of simulation along mortar head joints, the tensile stress was roughly 0.008 N/mm².

Table 4. Difference between mathematical and physical models' response along mortar head joints

Load step [mm]	Finite element size [mm]	f_{v0} [N/mm²]	Difference [%]
0.01	10	0.056	10.7
	20	0.054	7.4
	30	0.057	12.3
0.02	10	0.069	27.5
	20	0.064	21.9
	30	0.063	20.6

Table 5. Difference between computational and physical models' response along mortar bed joints

Load step [mm]	Finite element size [mm]	f_{v0} [N/mm²]	Difference [%]
0.01	10	0.239	7.9
	20	0.242	9.1
	30	0.241	8.7
0.02	10	0.243	9.5
	20	0.244	9.8
	30	0.242	9.1

5. Discussion of results

Appropriate specimens (physical models) were built in compliance with [7] in order to investigate shear strength of clay block masonry with mortar joint interlocking, i.e. f_v. The tests were carried out along the mortar head and bed joints, from which different behaviours were observed due to the influence of interlocking. Following determination of the most important physical model parameters involved, computational models were used in order to adequately present mortar interlocking in non-linear analyses of clay block masonry.
The initial shear strength of $f_{v0,h}$ = 0.05 N/ mm² and the coefficient of internal friction of μ_h = 0.45 were obtained during

tests conducted along mortar head joints, i.e., under three compressive stress values (f_p = 0.2, 0.6 and 1.0 N/mm^2). This was possible because the mortar head joint sliding occurred in all cases, i.e. there was no interlocking, unlike in case of solid bricks. In this instance, the shear strength remained as described in [1], i.e., $f_v = f_{v0} + \mu \cdot f_p$.

On the other hand, in tests conducted along mortar bed joints, the tensile strength of masonry units was reached before the mortar bed joint sliding could occur (which will not be the case for solid bricks). According to [7], this is considered unacceptable and should therefore be disregarded. In compliance with [1], the failure that occurred was considered as a limit to the shear strength value, i.e., $f_v = f_{vlt}$, and estimated using the expression $f_{vlt} = 0.065 \cdot f_{mu,c,h}$, where $f_{mu,c,h}$ is the masonry unit compressive strength normal to the bed face. However, several additional issues emerged:

- The expression for ultimate shear strength is applied only if the value obtained by $f_v = f_{v0} + \mu \cdot f_p$ exceeds this ultimate value, and not as the only option arising from the influence of interlocking (Figures 6 and 7)
- clay block tensile and compressive strength values, both normal and parallel to the bed faces, differ from each other (Table 1) due to the presence of voids (in our case, 68 % of the total volume)
- it was established that the expression $f_{mu,t,b} = 0.065 \cdot f_{mu,c,b}$, where $f_{mu,c,b}$ is the clay block compressive strength parallel to the bed face, corresponds well with the ultimate shear (tensile) stress obtained by testing.

When using the computational model to simulate the tests, clay blocks had to be modelled to include their physical properties in both parallel and normal to the bed face tests, respectively (Table 1). Clay block modelling is elaborated in detail in [13,14] and is therefore not considered in this paper. Additionally, the shear strength function had to be developed in order to include mortar interlocking in analyses (Figure 11). This was required because an interface material constitutive model based on Mohr-Coulomb friction was used. As a result, it was assumed that $f_{v0,b} = f_{v0,h}$, $\mu_b = \mu_h$ and $f_{t,b} = f_{t,h}$. The implementation of the shear resistance function as an addition to initial shear strength enabled accuracy of design model results, with the difference of 7.9 % with regard to test results. This was achieved by using a finite element mesh size of 10 mm and a prescribed displacement step of 0.01 mm, as determined by sensitivity analysis.

Modelled normal stresses of clay blocks in a near collapse state, shown in Figure 12, revealed the occurrence of tensile stresses at 0.75 N/mm^2, which exceeds the clay block tensile strength in the direction considered, i.e., $f_{mu,t,b}$ = 0.23 N/mm^2. This led to the cracking of clay blocks, which however differed from that observed in the physical model. These differences occurred due to the simplification of masonry units. Furthermore, because of the constitutive model used, cracks may occur but the masonry unit cannot separate (smeared-crack model). Tensile stresses of clay blocks in the test simulation along mortar head joints were negligible. Thus, the model provided an accurate response with regard to failure mechanism (10.7 % deviation for a finite element mesh size of 10 mm and a prescribed displacement step of 0.01 mm).

Due to the requirement specified in [2], mean physical properties were considered throughout the paper.

6. Conclusions

If clay blocks are used in masonry construction, interlocking occurs during placement of units and mortar, which is due to the presence of voids (usually along mortar bed joints as a result of construction practice). In earthquake-resistant design compliant with [1-3], the influence of interlocking on the shear strength of masonry is not recognized and thus not accounted for in the design process. Based on results obtained in the paper, the following conclusions and recommendations have been reached:

- interlocking causes tensile failure of masonry units rather than the mortar joint sliding during shear strength determination tests in compliance with [7]. This is an unavoidable failure mechanism and should not be disregarded, as stated in [7].
- clay blocks possess physical properties that are significantly different depending on whether they are normal or parallel to the bed face; therefore (also with respect to interlocking), clay block masonry cannot be treated in the same way as solid brick masonry in earthquake-resistant design. Additionally, the so-called pillow effect can occur due to weak physical properties of clay blocks parallel to bed faces, as described in [16].
- the shear strength of clay block masonry along mortar bed joints with interlocking will be taken as being equal to the masonry unit tensile strength parallel (not normal) to the bed face i.e. $f_v = f_{mu,t,b}$. The tensile strength can be adequately estimated using the expression $f_{mu,t,b} = 0.065 \cdot f_{mu,c,b}$, where $f_{mu,c,b}$ is the masonry unit compressive strength parallel to the bed face.

In non-linear analysis, the shear resistance function must be used in the constitutive model for interface material so as to supplement the initial shear strength along mortar joints with interlocking. However, to produce a valid structural design model, the clay block model has to be capable of capturing physical properties normal and parallel to the bed face. The shear strength function, i.e. the typical points in the function, must be verified by tests to determine not only the strength values but also the corresponding displacements.

Acknowledgements

The research presented in this paper is a part of the research project, "Framed-Masonry Composites for Modelling and Standardization", backed by the Croatian Science Foundation, whose support is gratefully acknowledged.

REFERENCES

[1] CEN: Eurocode 6: Design of masonry structures - Part 1-1: General rules for reinforced and unreinforced masonry structures (EN 1996-1-1:2005), European Committee for Standardization, Brussels, 2005.

[2] CEN: Eurocode 8: Design of Structures for Earthquake Resistance - Part 1: General Rules, Seismic Actions and Rules for Buildings (EN 1998-1:2004), European Committee for Standardization, Brussels, 2004.

[3] Sorić, Z.: Mechanical properties of nonreinforced masonry walls, Građevinar, 52 (2000) 2, pp. 67-78.

[4] Sigmund, V.: FRAmed-MAsonry Composites for Modelling and Standardization [Internet]. 2015 [cited 2015 Jan 13]. Available from: http://framed-masonry.com/

[5] CEN: Specification for masonry units - Part 1: Clay masonry units (EN 771-1:2011), European Committee for Standardization, Brussels, 2011.

[6] CEN: Methods of test for masonry units - Part 13: Determination of net and gross dry density of masonry units (except for natural stone) (EN 772-13:2000), European Committee for Standardization, Brussels, 2000.

[7] CEN: Methods of Test for Masonry - Part 3: Determination of Initial Shear Strength (EN 1052-3:2002/A1), European Committee for Standardization, Brussels, 2007.

[8] Cervenka Consulting s.r.o. ATENA for Non-Linear Finite Element Analysis of Reinforced Concrete Structures. Prague: Červenka Consulting s.r.o.; 2015.

[9] CEN: Methods of test for masonry units - Part 16: Determination of dimensions (EN 772-16:2011), European Committee for Standardization, Brussels, 2011.

[10] CEN: Methods of test for masonry units - Part 3: Determination of net volume and percentage of voids of clay masonry units by hydrostatic weighing (EN 772-3:1998), European Committee for Standardization, Brussels, 1998.

[11] CEN: Methods of test for mortar for masonry - Part 11: Determination of flexural and compressive strength of hardened mortar (EN 1015-11:1999/A1:2006), European Committee for Standardization, Brussels, 2006.

[12] Cervenka, V., Jendele, L., Cervenka, J.: ATENA Program Documentation Part 1 Theory, Cervenka Consulting Ltd., Prague, Czech Republic, 2012.

[13] Penava, D., Sigmund, V., Kožar, I., Anić, F., Trajber, D., Vig, M.: Influence of 2D and 3D Micro Modelling Approach in Seismic Design of Framed-Masonry Structures with Respect to Hollow Clay Masonry Units, 3rd Aachen Conference on Computational Engineering Science (ACCES), Aachen, Germany, 2015.

[14] Penava, D., Sigmund, V., Kožar, I., Anić, F., Trajber, D., Vig, M.: Spatial micro model of the masonry wall, 8th International Congress of Croatian Society of Mechanics, Opatija, Croatia, 2015.

[15] Necevska-Cvetanovska, G., Sendova, V., Apostolska, R.: Frame - Masonry Composites for Modelling and Standardization (Framed-Masonry) Report IZIIS 2015 - 31, Skopje, Macedonia, 2015.

[16] Sigmund, V., Penava, D.: Influence of openings, with and without confinement, on cyclic response of infilled r-c frames - an experimental study, Journal of Earthquake Engineering, 18 (2014) 1, pp. 113-46, http://dx.doi.org/10.1080/13632469.2013.817362